[AMERICAN JOURNAL OF SCIENCE, VOL. 260, MAY 1962, P. 321-336]

American Journal of Science

MAY 1962

THE DYNAMIC SIGNIFICANCE OF DEFORMATION LAMELLAE IN QUARTZ OF A CALCITE-CEMENTED SANDSTONE

EDWARD HANSEN* and IRIS Y. BORG**

Department of Geology, Princeton University, Princeton, New Jersey

ABSTRACT. In three specimens of macroscopically folded Oriskany sandstone, deformation lamellae are profusely developed in quartz grains, and the calcite cement contains numerous twin lamellae on $\{01\bar{1}2\} = e$. Following the method used by Turner (1953), "axes of compression and tension" were deduced from a statistical study of the pattern of calcite twinning in each specimen. The stress systems so deduced are symmetrically related to the geometry of macroscopic folding. Triaxial stress fields were obtained from samples from the limbs of an anticline, and a uniaxial stress field was determined from a sample from the axial plane of the anticline. The maximum and minimum stress axes, σ_1 and σ_3, so determined lie within 10° of the bedding and are perpendicular to the local fold axis; the intermediate axis, σ_2, parallels the fold axis. Quartz lamellae show strong patterns of preferred orientation also symmetrically related to the stress systems deduced from calcite twinning; they tend preferentially to develop in planes of high shear stress inclined at less than 45° to the inferred axis of maximum stress, σ_1.

INTRODUCTION

In 1958 when this study was made, the significance of lamellae in quartz had remained elusive, despite numerous investigations starting in the last century. Because of the preponderance of these structures in deformed quartzites, it seemed likely that they arose subsequent to crystallization through purely mechanical means; hence the common term "deformation lamellae". It has long been known that quartz lamellae of tectonites show a high degree of preferred orientation, and for this reason some writers (Schmidt, 1927; Hietanen, 1938) considered them to be glide planes, conclusions scarcely warranted because other kinds of discontinuities, such as fractures, cleavages, and even deformation bands, as rigorously defined by metallurgists, may show a similarly high degree of orientation without themselves being planes of slip. Attempts have been made to relate patterns of quartz lamellae to stress fields inferred from other structures in the same rock. For example, Naha (1959) has shown that lamellae in quartz make angles of 45° to 57° to the minimum principal stress deduced from tension cracks in associated garnet. Yet experimental efforts to produce them in artificially deformed quartz had all failed (Griggs and Bell, 1938; Fairbairn, 1950; Borg and Maxwell, 1956).

Turner and Chi'h (1951, p. 897-900) showed that during minor experimental strain of Yule marble there is a close correlation between development of abundant $\{01\bar{1}2\}$ twin lamellae in calcite and the orientation of the lamellae with respect to the axes of loading. On the assumption that a similar relation holds in naturally strained marbles, Turner (1953) used the pattern of

* Present address: Department of Geology, Yale University, New Haven, Connecticut.
** Present address: Department of Geology, University of California, Berkeley, California.

observed {01$\bar{1}$2} twin lamellae in several specimens of marble to locate "compression and tension axes" (also termed "a simple system of applied stress"). The deduced axes have subsequently been found to be consistently oriented throughout relatively large domains (McIntyre and Turner, 1953; Clark, 1954), and they are thought to represent a stress system imposed in the last stages of deformation of the rocks in question.

Using Turner's technique we have examined lamellae in quartz in the light of information garnered from patterns of {01$\bar{1}$2} twin lamellae in the calcite cement of the Oriskany sandstone. The results and methods used in the study constitute the present report. They have been briefly reported in abstract (Hansen, Borg, and Maxwell, 1959). Two developments in the intervening years have caused us to present the data more fully: (1) Deformation lamellae in quartz have been produced experimentally (Carter, Christie, and Griggs, 1961) under stress conditions compatible with the information provided by this study. (2) Several investigators, e.g. Christie and Raleigh (1959) and Melvin Friedman (1960, personal communication), also using Turner's method, have attacked the same problem, and their data and interpretations are so varied that it is clear that there is a need for additional detailed information on the relation between deformational features of quartz and associated calcite in common rocks.

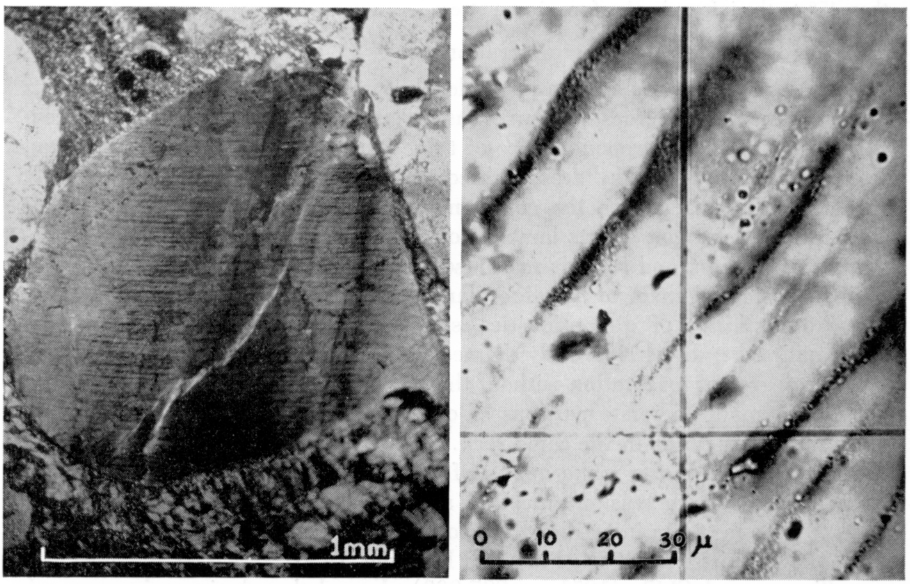

Fig. 1 Fig. 2

PLATE 1

Photomicrographs of lamellae in quartz grains from the Oriskany sandstone.

Fig. 1. Well developed lamellae subnormal to zones of undulatory extinction. Crossed nicols.

Fig. 2. Lamellae at high magnification inclined at 75° to 80° to the plane of the photograph. Crossed nicols.

observed {01$\bar{1}$2} twin lamellae in several specimens of marble to locate "compression and tension axes" (also termed "a simple system of applied stress"). The deduced axes have subsequently been found to be consistently oriented throughout relatively large domains (McIntyre and Turner, 1953; Clark, 1954), and they are thought to represent a stress system imposed in the last stages of deformation of the rocks in question.

Using Turner's technique we have examined lamellae in quartz in the light of information garnered from patterns of {01$\bar{1}$2} twin lamellae in the calcite cement of the Oriskany sandstone. The results and methods used in the study constitute the present report. They have been briefly reported in abstract (Hansen, Borg, and Maxwell, 1959). Two developments in the intervening years have caused us to present the data more fully: (1) Deformation lamellae in quartz have been produced experimentally (Carter, Christie, and Griggs, 1961) under stress conditions compatible with the information provided by this study. (2) Several investigators, e.g. Christie and Raleigh (1959) and Melvin Friedman (1960, personal communication), also using Turner's method, have attacked the same problem, and their data and interpretations are so varied that it is clear that there is a need for additional detailed information on the relation between deformational features of quartz and associated calcite in common rocks.

Fig. 1

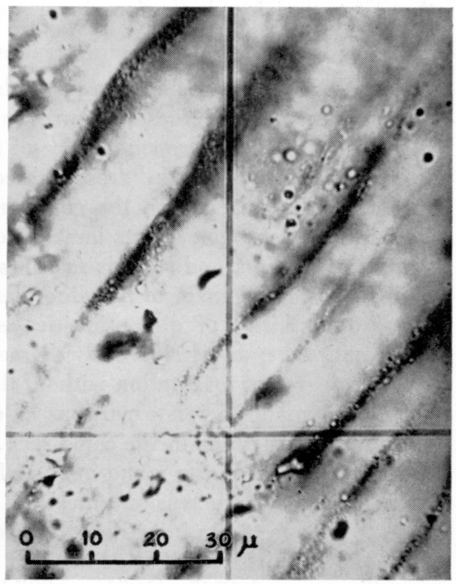

Fig. 2

PLATE 1

Photomicrographs of lamellae in quartz grains from the Oriskany sandstone.

Fig. 1. Well developed lamellae subnormal to zones of undulatory extinction. Crossed nicols.

Fig. 2. Lamellae at high magnification inclined at 75° to 80° to the plane of the photograph. Crossed nicols.

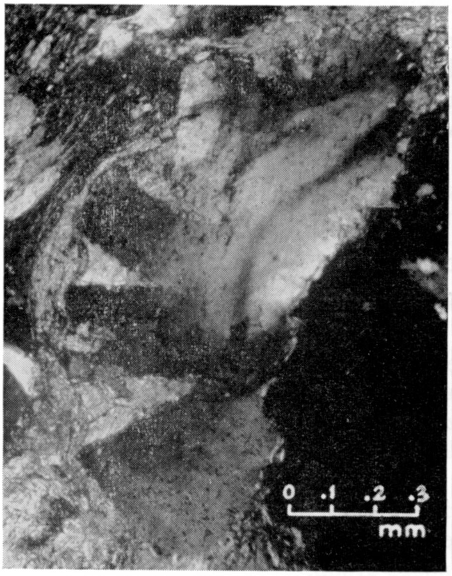

Fig. 1

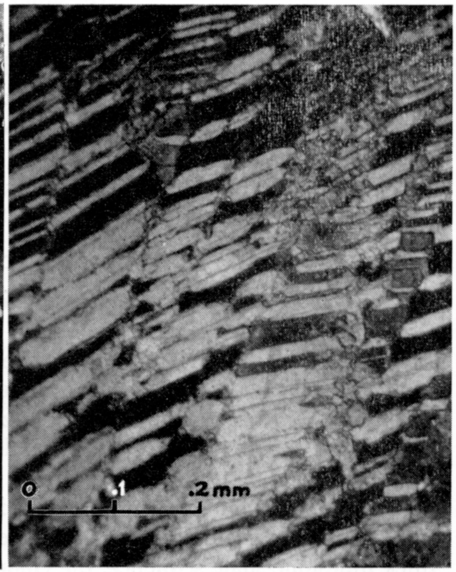

Fig. 2

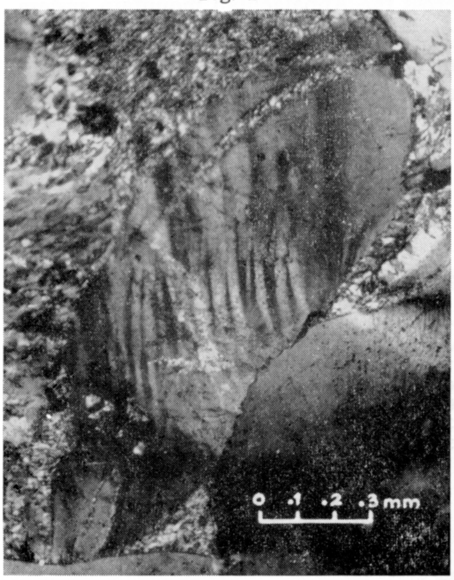

Fig. 3

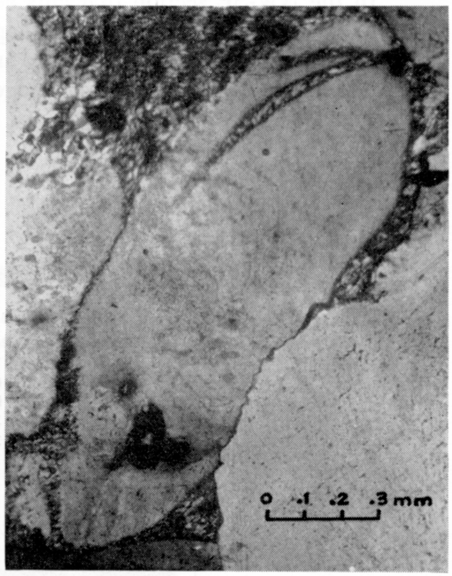

Fig. 4

PLATE 2

Photomicrographs of deformational microstructures in calcite and quartz from the Oriskany sandstone.

Fig. 1. A bent quartz grain showing undulatory extinction and (at left) peripheral tension fractures filled by calcite. Crossed nicols.

Fig. 2. Calcite highly twinned on *e* $\{01\bar{1}2\}$. Crossed nicols.

Fig. 3. Extinction bands subparallel to [0001] in quartz; lamellae can be seen nearly perpendicular to the bands. Crossed nicols.

Fig. 4. The same grain as in figure 3. Plane polarized light.

ACKNOWLEDGMENTS

We wish to thank the Department of Geology and John C. Maxwell of Princeton University for support of the research. F. J. Turner has aided us through profitable discussion and editorial comment. We are also indebted to A. De, who made available his and A. K. Saha's data (at present published only in abstract form) relating to the crystallographic orientation of lamellae in quartz. Professor Matt Walton of Yale University generously made possible the completion of the drafting through the loan of his draftsman.

GEOLOGIC SETTING

Samples of the lower Devonian Oriskany sandstone were collected approximately one mile west of the village of Delaware Water Gap in eastern Pennsylvania. There the Oriskany sandstone is 60 feet thick and consists of massive quartz arenite interlayered with siliceous limestone. The massive beds are composed of well rounded grains of quartz and chert, with a few scattered microcline grains, cemented with calcite, dolomite, chalcedony, quartz, and chert in varying proportions. Specimens were chosen from the quartz arenite beds whose chief cement is calcite. Underlying the Oriskany sandstone is over 500 feet of Helderberg limestone and shale; the Oriskany is overlain by another thick limestone-shale sequence, the Onondaga group.

In the NW-SE section that cuts across the Appalachian mountain system and includes the Delaware Water Gap region, the outcrops of the Oriskany sandstone lie in the outermost Valley and Ridge fold—the Godfrey Ridge anticline; north and west of Godfrey Ridge, the Paleozoic rocks display the gentle

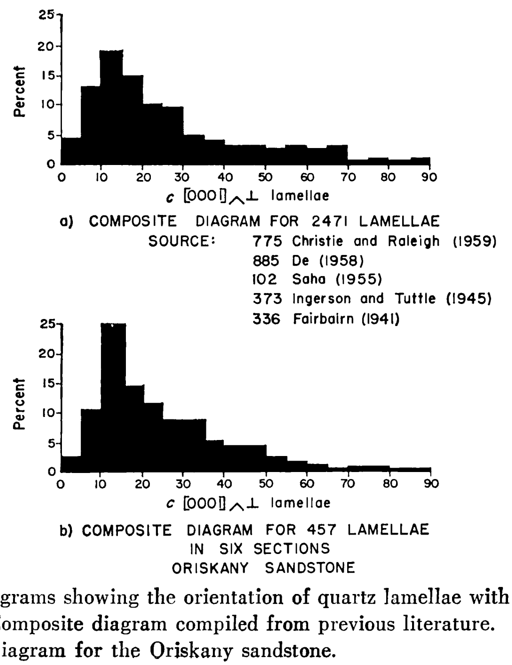

Fig. 1. Histograms showing the orientation of quartz lamellae with respect to [0001].
A. Composite diagram compiled from previous literature.
B. Diagram for the Oriskany sandstone.

dips characteristic of the Cumberland Plateau. The anticline at Godfrey Ridge is slightly overturned toward the northwest, and beds of the northwestern limb locally attain vertical dips. The limestone-shale sequence displays moderately well developed, axial-plane cleavage, but the few beds of massive Oriskany sandstone within this sequence show no such megascopic structures and appear to have acted as competent units within an otherwise incompetent mass.

The three samples studied in detail come from a section through the Godfrey Ridge anticline. E2 was collected at the axial plane of the fold; E4 was taken from the southeastern, nearly flat-lying limb; and E6 from the steep northwestern limb.

NATURE OF QUARTZ LAMELLAE IN THE ORISKANY SANDSTONE

The observed quartz lamellae (pl. 1) differ in no significant way from those described by Hietanen (1938), Fairbairn (1941), and Ingerson and Tuttle (1945). Figure 1 of plate 1 is a highly undulatory grain containing profuse lamellae; figure 2 illustrates lamellae at high magnification and inclined at 75° to 80° to the plane of the photograph. The darkening along the trend of the lamellae is due to impurities that have perhaps diffused to dis-

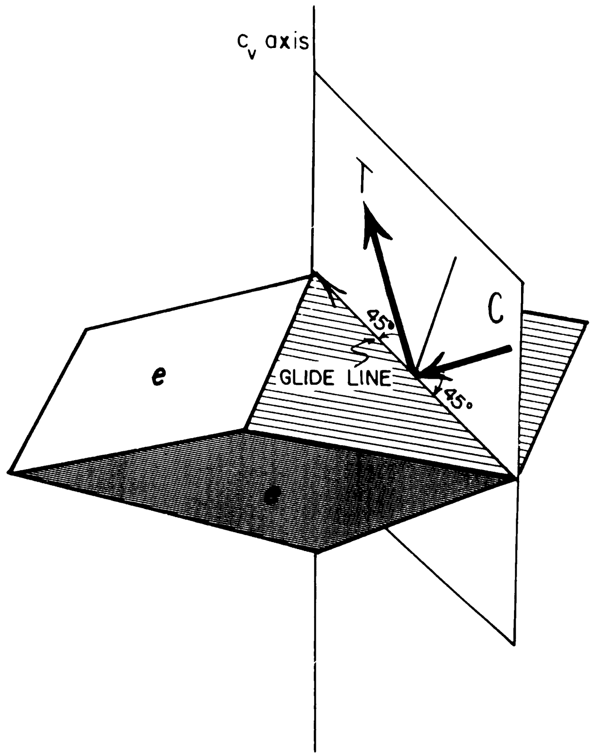

Fig. 2. Geometry of twin gliding on the negative rhombohedron e $\{01\bar{1}2\}$ in calcite. The deduced maximum optimum principal stress axis (C) and the minimum principal stress axis (T) lie in the deformation plane at 45° to the twin plane; C, T, [0001], and the normal to e are coplanar.

continuities formed by lamellae boundaries. Inclusions occur throughout, and inspection of the inclined surface of the lamellae reveals a granular texture, which suggests a high concentration of very small inclusions on the planes. Note also the nonplanar nature of the discontinuities as shown by their undulating trend and by variation in their apparent width. The width of the individual lamella is estimated from figure 2 of plate 1 to be less than 0.8μ, and the spacing between them to be 8 to 24μ, which is of the same order of magnitude as Riley's estimate of 2.5 to 17μ (1947, p. 462). The range of crystallographic orientation of quartz lamellae (fig. 1B) is essentially the same as that recorded in other quartz tectonites (fig. 1A). The two histograms of figure 1 are nearly identical, the only difference being the greater concentration (5 percent) at 10° to 15° in the Oriskany than in quartz studied previously.

Plate 2 illustrates various microscopic deformational structures associated with quartz lamellae in the Oriskany sandstone: In figure 1 a bent quartz grain shows strong undulatory extinction and peripheral V-shaped tension fractures filled by calcite cement. Figure 2 illustrates the well developed *e* twinning in calcite. In figure 3 quartz lamellae are associated with banding parallel to the *c* axis. Grain contacts are more clearly shown in figure 4.

STRESS SYSTEMS DEDUCED FROM GEOMETRY OF CALCITE GLIDE

The technique used to determine the stress field from the incidence of $\{01\bar{1}2\}$ twinning in calcite is well described in the literature by Turner (1953), McIntyre and Turner (1953), and Clark (1954). In brief, conditions

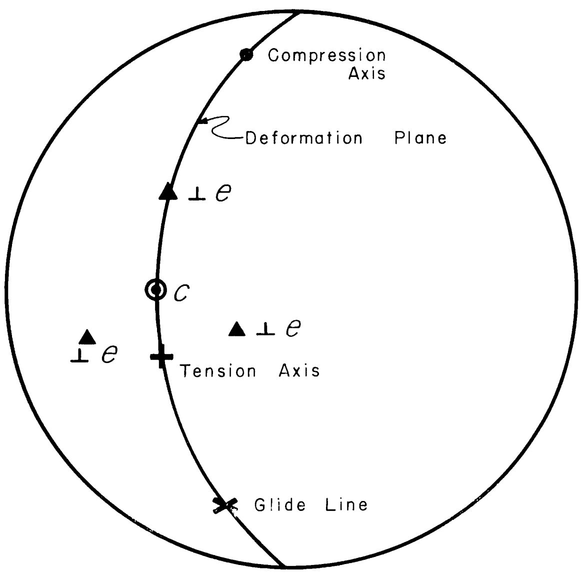

Fig. 3. Relation of deduced stress axes, C and T, to the twin plane, *e*, *c* axis, and the glide line in calcite, shown in lower hemisphere, equal-area projection.

$\perp e \wedge$ [0001] = 26°	[0001] $\wedge$ Compression axis = 71°
$\perp e \wedge$ Compression axis = 45°	[0001] $\wedge$ Tension axis = 19°
$\perp e \wedge$ Tension axis = 45°	[0001] $\wedge$ glide line = 64°

for simple glide are theoretically optimum when both the glide plane and the glide line are inclined at 45° to both the maximum and the minimum stresses —σ_1 and σ_3; the resolved shear stress coefficient, S_o, then has the maximum value 0.5. Since the sense of twin gliding on {01$\bar{1}$2} in calcite is unique (fig. 2), it is possible in any twinned grain to locate a maximum principal stress axis (σ_1 = C) and a minimum principal stress axis (σ_3 = T) that define the optimum stress system for twinning. These directions are shown in figures 2 and 3, inclined respectively at 71° and 19° to [0001] in the plane which con-

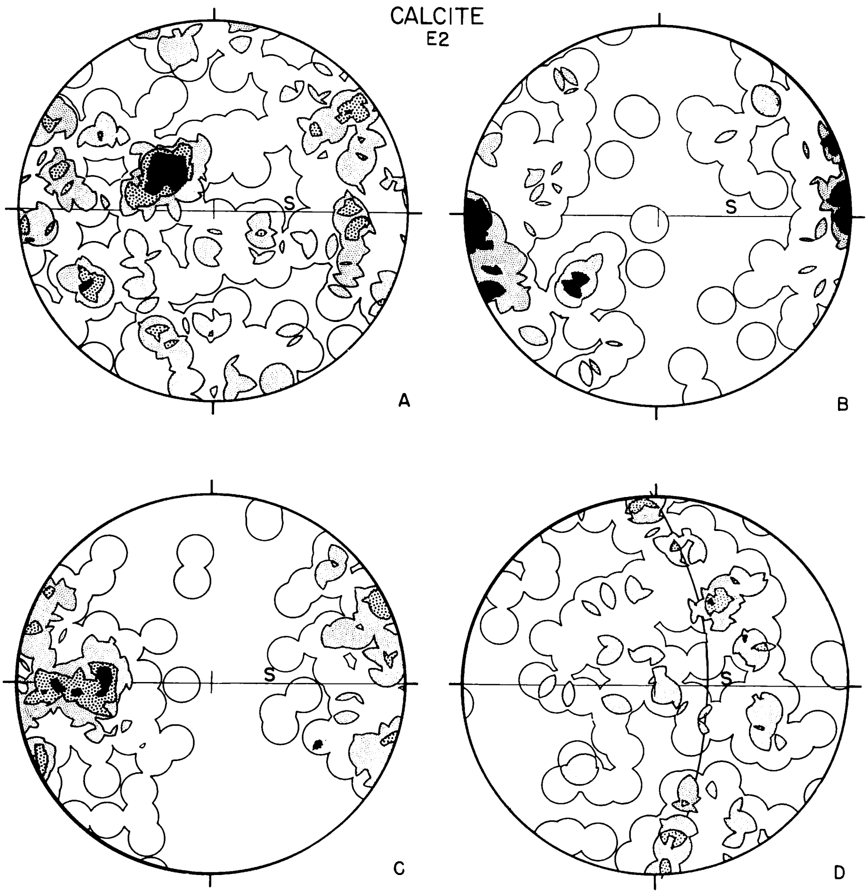

Fig. 4. Calcite data from specimen E2. Bedding: strike N40°E, dip 45°NW.
A. *c* axes of 200 grains (100 grains from each of two mutually perpendicular thin sections rotated into coincidence). Bedding, s, is indicated by great circle. Contours: 0.5, 1.5, 2.5, 3.5% per 1% area; maximum 5%.
B. Poles to 118 well developed {01$\bar{1}$2} twin lamellae from the 200 grains of A above. Contours: 0.9, 2.6, 4.3% per 1% area; maximum 9.4%.
C. Compression axes computed for each of the 118 twins of diagram B. Contours: 0.9, 2.6, 4.3, 6.0% per 1% area; maximum 6.8%.
D. Tension axes computed for each of the 118 twins of diagram B. Contours: 0.9, 2.6, 4.3, 6.0% per 1% area; maximum 6.0%. Great circle indicates the trend of the plane containing axes.

tains the normal to the glide plane, the glide line, and [0001]. The stress axes for the rock as a whole are identified with concentrations of individual σ_1 and σ_3 axes determined in each of a large number of twinned grains.

This kind of analysis involves two implicit assumptions, neither of which necessarily holds good for every individual grain: (1) Observed $\{01\bar{1}2\}$ twins are the result of crystal gliding, not of growth. (2) The host grain represents

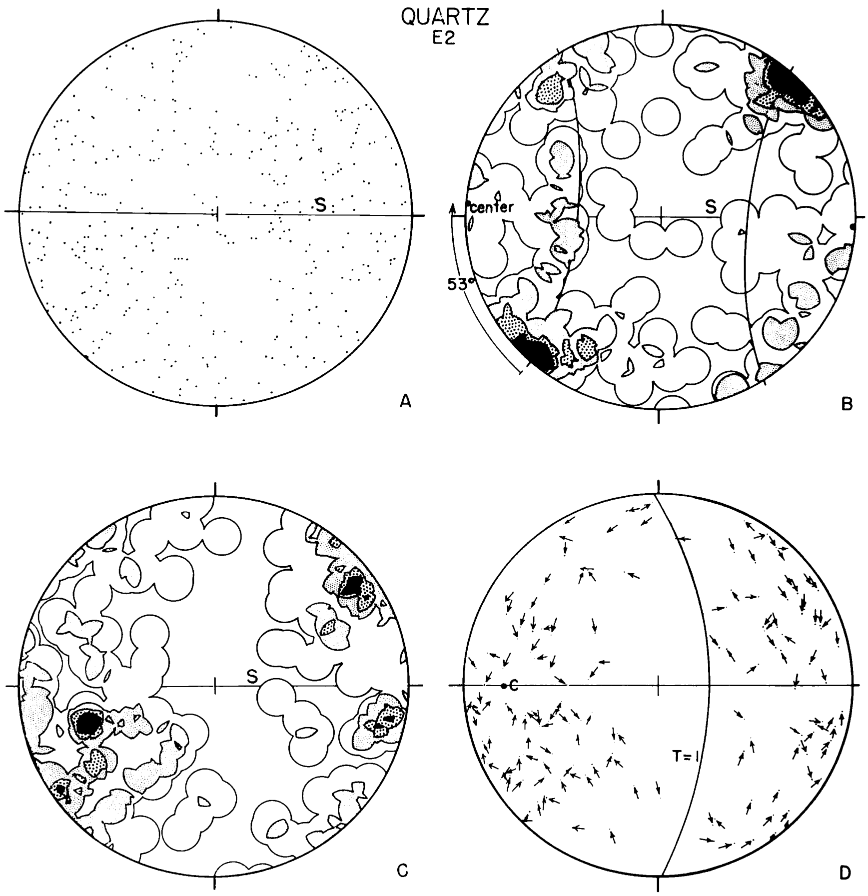

Fig. 5. Quartz data from specimen E2. Bedding: strike N40°E, dip 45° NW.

A. *c* axes of 400 grains (200 grains from each of two mutually perpendicular thin sections rotated into coincidence). Bedding is shown as a great circle marked s.

B. Poles to 147 lamellae from the 400 grains of A above. The small circle of 53° radius defined by poles to lamellae is marked with a dot at its center. Contours: 0.7, 2.1, 3.5, 4.9, 6.3% per 1% area; maximum 8.4%.

C. *c* axes of 147 grains containing the lamellae of diagram B. Contours: 0.7, 2.1, 3.5, 4.9% per 1% area: maximum 6.3%.

D. Arrows are portions of the great circles connecting the *c* axis and the pole to the lamella for each of the 147 lamellae of diagram B. Arrows point to the *c* axis of the enclosing grain. C marks the compression axis determined from calcite data of figure 4C. The great circle T = I represents the plane containing the tension axes determined from calcite data presented in figure 4D.

the initial lattice and that enclosed by the lamellae is the twinned counterpart. Where most grains contain relatively few lamellae, it is likely that deformation is in the incipient stage so that the second assumption at least is valid. There is also the problem as to whether the strain recorded in the pattern of calcite twinning can be correlated with that expressed by associated lamellae in quartz and also with the gross deformation of the rock as a whole. These questions can only be resolved by the totality of the data available for each specimen or locale.

METHOD OF MICROSCOPIC ANALYSIS

For most specimens two thin sections cut mutually perpendicular to each other and to the bedding of the sandstone were examined with a universal stage. The data for each specimen have been rotated into coincidence and contoured together on a single petrofabric diagram projected from the lower hemisphere onto an equal-area net. This procedure eliminates the "central blind spot" that occupies the middle of any projection of data for planar structures compiled in a single section. However, sampling errors are also inherent in a compilation of data from mutually perpendicular sections, each with its "blind spot". Depending on whether two or three sections are used, the composite diagram contains one or three areas that have been sampled twice. The petrofabric diagrams in this paper have this defect, but in no instance do maxima coincide with an area of overlapping sampling; in fact, the areas of overlap happen to lie between maxima which thus tend to be artificially weakened.

RESULTS OF ANALYSES

Specimen E2

Calcite.—Figure 4A shows the distribution of *c* axes in 100 grains from each of two thin sections rotated into coincidence and plotted together. Poles to 117 well developed $\{01\bar{1}2\}$ twin lamellae in the same 200 grains are shown in figure 4B. Figures 4C and D contain contoured compression and tension points (σ_1 and σ_3, respectively) calculated for each of the $\{01\bar{1}2\}$ lamellae. The compression points are grouped in a point maximum, and the tension points are unevenly distributed along a great circle 90° distant from this. In the absence of a clearly defined maximum of tension axes, σ_1 is greater than σ_2 which equals σ_3, and the stress field so deduced has axial symmetry. This stress system has previously been found to be associated with conical distribution of fractures in artificially deformed sands (Borg and Maxwell, 1956, p. 75) rather than with sets of conjugate planar shears.

Quartz.—The orientation of *c* axes in the 400 grains measured approaches randomness (fig. 5A); in contrast, the *c* axes of the 147 grains containing lamellae show a fair degree of preferred orientation (fig. 5C), as has been demonstrated in previous investigations (Ingerson and Tuttle, 1945; Christie and Raleigh, 1959). Poles to the lamellae in figure 5B show an even higher degree of orientation. They are unevenly distributed along small circles of 53° radius; the planes, therefore, are tangent to a cone whose semi-apex angle is about 37°. The axis of the cone (marked "center" in figure 5B) lies near the bedding plane, *s*. Comparison with the calcite data shows that the axis of this cone lies approximately 10° from the point maximum defined by the compression axes (σ_1) in figure 4C. As σ_2 equals σ_3 in the stress field deduced statistically from calcite, it is not surprising that the distribution of quartz lamellae in this rock approaches axial symmetry by defining a cone about σ_1. Figure 5D shows a portion of the great circle containing the *c* axis and the normal to lamellae for each of the 147 measured sets of lamellae in quartz. By convention the arrows point to the *c* axis of the enclosing grain. There is a striking tendency for the arrows to point toward the cone axis (σ_1). The symmetry of

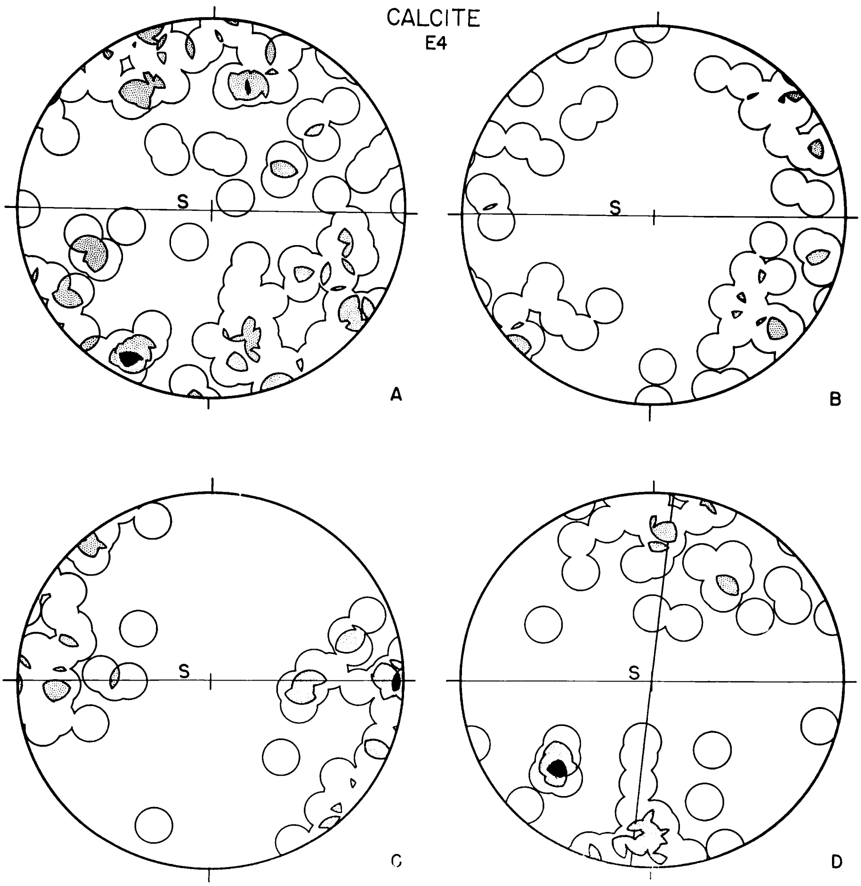

Fig. 6. Calcite data from sample E4. Bedding: strike E-W, dip 12°S.

A. *c* axes of 100 grains from a single thin section. Bedding is shown as a great circle marked s. Contours: 1, 3, 5% per 1% area; maximum 6%.

B. Poles to 49 well developed {01$\bar{1}$2} twins from the 100 grains of diagram A. Contours: 2, 6% per 1% area; maximum 7%.

C. Compression axes computed for each of the 49 twin lamellae of B above. Contours: 2.6, 10% per 1% area; maximum 10%.

D. Tension axes computed for each of the 49 lamellae in diagram B. Great circle trending *ca.* N-S is plane normal to C containing T and I. Contours: 2, 6, 10%; maximum 10%.

the quartz lamellae pattern correlates with that of the stress field deduced from calcite twinning.

Specimen E4

Calcite.—Measurements on calcite were restricted to a single thin section. Figures 6A and B show the distribution of 100 *c* axes and 49 poles to well developed {01$\bar{1}$2} lamellae, respectively. Both diagrams show low orders of pre-

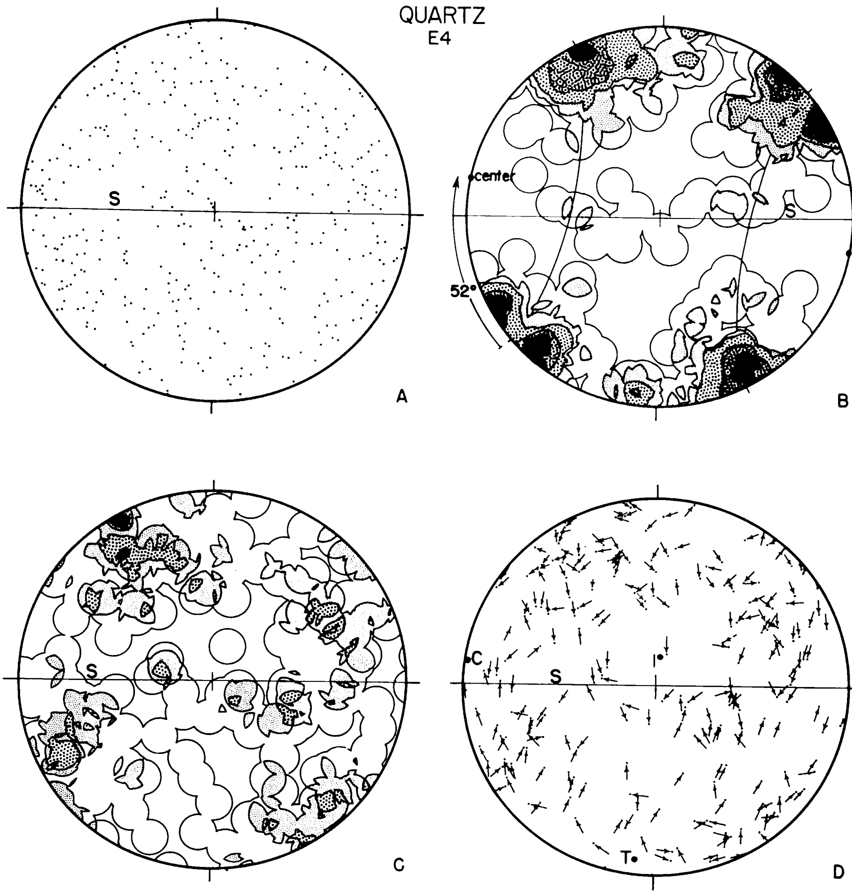

Fig. 7. Quartz data from specimen E4. Bedding: strike E-W, dip 12°S.

A. *c* axes of 412 grains from two mutually perpendicular thin sections rotated into coincidence. Bedding, s, is shown as a great circle.

B. Poles to 220 lamellae from the 412 grains of diagram A. The small circle of 52° radius defined by poles to lamellae is marked with a dot at its center. Contours: 0.5, 1.4, 2.3, 3.6, 5.0% per 1% area: maximum 7.3%.

C. *c* axes of 193 grains containing the lamellae of diagram B. Contours: 0.5, 1.6, 2.6, 3.7% per 1% area; maximum 4.1%.

D. Arrows are portions of the great circles connecting the *c* axis and the pole to lamellae for each of the 220 lamellae of diagram B. Arrows point to the *c* axis of the enclosing grain. C, I, and T mark the compression, intermediate, and tension axes, respectively, determined from calcite data presented in figures 6C and D.

ferred orientation. Compression and tension points graphically constructed for the 49 highly twinned grains show concentrations into discrete maxima (figs. 6C and D). The center of gravity of the compression axes (σ_1) lies about 10° from the bedding, and the maximum of the tension axes (σ_3) lies 90° from the compression maximum and approximately 80° to 85° from the bedding. The stress field so constructed is triaxial.

Quartz.—*c* axes of 412 grains in two sections are shown in figure 7A; as in specimen E2 (fig. 5A), they have nearly random distribution. The 193 grains containing lamellae, however, show a definite preferred orientation (fig. 7C), and the lamellae show an even stronger pattern (fig. 7B). Statistically they tend to lie in two planes that make an angle of 75° to 80° to each other and intersect near the bedding plane. The approximate position of the bisector of that acute angle is indicated on figure 7B by "center". It is skewed from the bedding plane by about 10° and in a direction identical to that of the compression maximum (σ_1) obtained from calcite (fig. 6C); in fact, these points from the two diagrams are coincident. In contrast to the lamellae in E2 (fig. 5B), there is only a hint at conical development about the "center" point. A plot of the great circle containing [0001] and the pole to lamellae (fig. 7D) shows less regularity than the comparable one for specimen E2 (fig. 5D). The only evident tendency is for the arrows to point toward a plane that is nearly parallel to the bedding and defined by σ_1 (C) and σ_2 (I) of the stress field.

Specimen E6

Calcite.—Figure 8A shows the distribution of *c* axes in 134 grains from two mutually perpendicular sections. Poles to 92 well developed $\{01\bar{1}2\}$ twins from the same 134 grains are shown in figure 8B. Compression and tension axes computed for each of the 92 *e* lamellae are presented in figures 8C and D, respectively. The compression points are grouped in a rather broad, point maximum, which centers within the bedding. The tension points are grouped in a similar broad, point maximum, which is located about 90° away from both the compression maximum and the bedding. The stress field deduced from these data is triaxial, $\sigma_1 > \sigma_2 > \sigma_3$, similar to that deduced for specimen E4.

Quartz.—The *c* axes of 210 grains from two sections are plotted in figure 9A; as in the previous two samples, the preferred orientation is weak. The 85 grains containing lamellae show only a slightly better preferred orientation of *c* axes (fig. 9C), but poles to the 92 sets of lamellae show a stronger pattern (fig. 9B). The two maxima indicate two statistically defined planes (comparable to those in E4, figure 7B) which make an acute angle of about 60° to 70° to each other and intersect near the bedding. An arbitrary small circle containing the maxima is drawn about the point marked "center", thereby bringing that point into close proximity to the concentration of compression axes of figure 8C. In this instance there is some justification for the interpretation, as both E2 and E4 (see figs. 5B and 7B) demonstrate the relation in less equivocal fashion. However, without the supporting data of adjacent samples and associated twinned calcite, diagrams such as figure 9B at present could not be used to locate stress axes exactly. If artificially produced lamellae in quartz are indeed restricted to planes at angles less than 45° to σ_1, the angle between maxima in diagrams such as figure 9B could be used to designate general areas that must contain σ_1, σ_2, and σ_3.

The plot of the great circle containing [0001] and the pole to a set of lamellae (fig. 9D) is comparable in its irregularity to the diagram for specimen E4 (fig. 7D); here also the only tendency is for arrows to point toward the plane defined by σ_1 (C) and σ_2 (I).

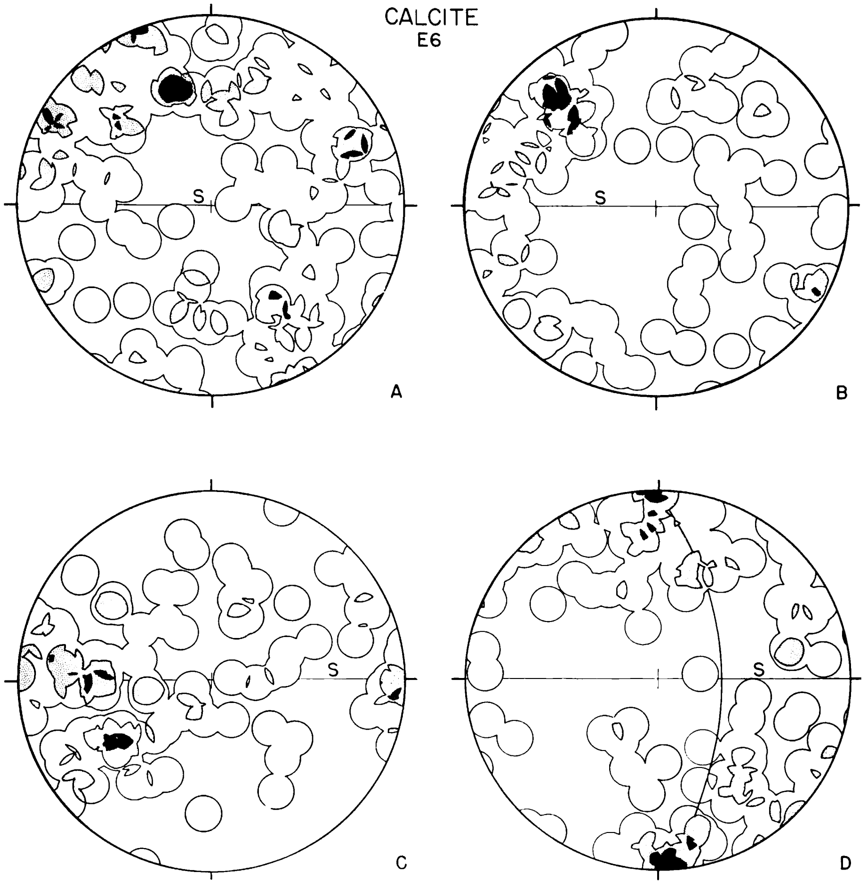

Fig. 8. Calcite data from specimen E6. Bedding: strike N70°E, dip 69°N.

A. *c* axes of 134 grains from two mutually perpendicular thin sections rotated into coincidence. Bedding, s, is shown as a great circle. Contours: 0.7, 2.2, 3.8% per 1% area; maximum 5.2%.

B. Poles to 92 well developed {01$\bar{1}$2} twin lamellae from the 134 grains of diagram A. Contours: 1.1, 3.3, 5.5% per 1% area; maximum 7.6%.

C. Compression axes computed for each of the 92 twin lamellae in diagram B. Contours: 1.1, 3.3, 5.5% per 1% area; maximum 7.6%.

D. Tension axes computed for each of the 92 lamellae in diagram B. Contours: 1.1, 3.3, 5.5% per 1% area; maximum 8.7%. Great circle is the plane normal to maximum of figure 8C containing T and I.

DYNAMIC SYNTHESIS

Traces of bedding planes measured at six localities on the Godfrey Ridge anticline are plotted as great circles in figure 10. The locus of their intersections, β, defines statistically the fold axis, B, which trends N70°E and plunges a few degrees toward the southwest.

Solid circles are compression axes, σ_1, deduced from calcite lamellae; crosses are tension axes σ_3; solid triangles represent the intermediate axes, σ_2,

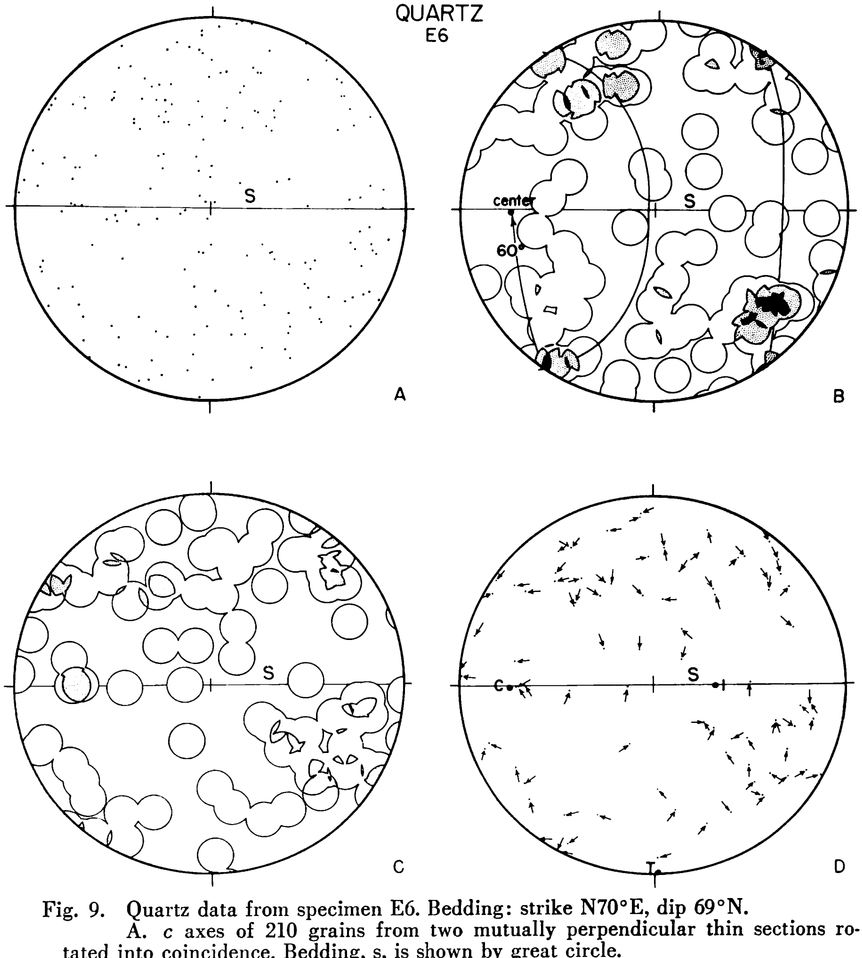

Fig. 9. Quartz data from specimen E6. Bedding: strike N70°E, dip 69°N.

A. *c* axes of 210 grains from two mutually perpendicular thin sections rotated into coincidence. Bedding, s, is shown by great circle.

B. Poles to 92 lamellae from the 210 grains of diagram A. An arbitrary circle of 60° radius containing the maxima is marked with a dot at its center. Contours: 1.1, 3.3, 5.5% per 1% area; maximum 5.9%.

C. *c* axes of 85 grains containing the lamellae in diagram B. Contours: 1.2, 3.5, 5.9% per 1% area; maximum 5.9%.

D. Arrows are portions of the great circles connecting the *c* axis and the pole to the lamella for each of the 92 lamellae of diagram A. Arrows point to the *c* axis of the enclosing grain. C, I, and T mark compression, intermediate and tension axes, respectively, determined from calcite data of figures 8C and D.

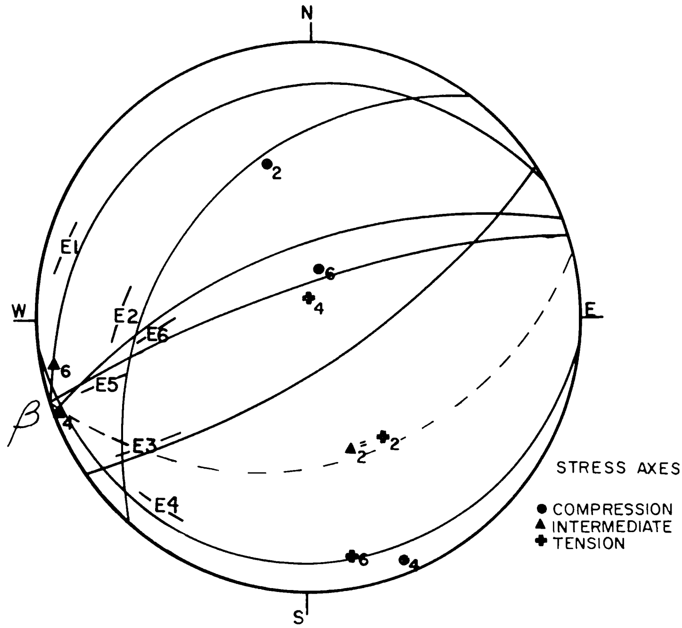

Fig. 10. β-diagram for bedding in folded Oriskany sandstone. Traces of individual measured bedding planes (E1, etc.) are plotted as great circles on an equal-area projection (lower hemisphere) on the geographic horizontal plane. Stress system deduced from calcite lamellae: full circles, compression axes, σ_1; crosses, tension axes, σ_3; full triangles, intermediate axes, σ_2; subscripts refer to specimen numbers.

normal to σ_1 and to σ_3; subscripts refer to specimen numbers. For specimen E2, in which the tension axes are spread uniformly in a girdle, this is represented by a broken arc with notation showing $\sigma_2 = \sigma_3$. Although the principal axes of the stress system are oriented differently in different domains within the fold, they nevertheless show three remarkably regular features:

(1) σ_1 and σ_3 lie normal to, and σ_2 coincides with, the fold axis, $\beta = B$. The same relation was found by McIntyre and Turner (1953, p. 239-240) in their study of calcite twinning in marbles from northeastern Scotland.

(2) The symmetry of the overall stress system coincides precisely with that of the fold.

(3) σ_1 in all three specimens is inclined at less than 10° from the bedding, the sense of departure being the same in all three. "Unrolling" of the bedding about β would give a uniform stress system with σ_1 inclined at about 10° to the horizontal bedding plane. This is consistent with, but does not prove, structural evolution in the two stages described thus: (1) Development of calcite lamellae in response to a subhorizontal compression along an axis trending N20°W—normal to β; (2) folding under continued compression in the same direction with passive rotation of the calcite fabric to its present orientation. Alternatively the calcite lamellae reflect locally varying stress fields synchronous with folding and conforming to the symmetry of the fold.

The symmetrical relation of quartz lamellae to the stress fields deduced from calcite lamellae suggests that both kinds of structures developed simultaneously under the same stress system. In conformity with the findings of Carter, Christie, and Griggs (1961) regarding experimental development of lamellae in quartz, the quartz lamellae in the Oriskany sandstone formed preferentially in planes of high shear stress; these are inclined at *less than 45°* to the principal stress axis, σ_1, deduced from associated calcite lamellae. In the absence of calcite, the orientation of quartz lamellae might therefore eventually be used to deduce the stress system under which they formed.

References

Borg, I. Y., and Maxwell, J. C., 1956, Interpretation of fabrics of experimentally deformed sands: Am. Jour. Sci., v. 254, p. 71-81.

Carter, N. L., Christie, J. M., and Griggs, D. T., 1961, Experimentally produced deformation lamellae and other structures in quartz sand [abs.]: Jour. Geophys. Research, v. 66, p. 2518-2519.

Christie, J. M., and Raleigh, C. B., 1959, The origin of deformation lamellae in quartz: Am. Jour. Sci., v. 257, p. 385-407.

Clark, R. H., 1954, A study of calcite twinning in the Strathavon marble, Banffshire: Geol. Mag., v. 91, p. 121-128.

De, Aniruddha, 1958, Observations on the deformation lamellae in quartz of four Indian tectonites [abs.]: Am. Geophys. Union Trans., v. 39, p. 512.

Fairbairn, H. W., 1941, Deformation lamellae in quartz from the Ajibik formation, Michigan: Geol. Soc. America Bull., v. 52, p. 1265-1277.

——— 1950, Synthetic quartzite: Am. Mineralogist, v. 35, p. 735-748.

Griggs, D. T., and Bell, J. F., 1938, Experiments bearing on the orientation of quartz in deformed rocks: Geol. Soc. America Bull., v. 49, p. 1723-1746.

Hansen, E. C., Borg, I. Y., and Maxwell, J. C., 1959, Dynamic significance of quartz lamellae [abs.]: Jour. Geophys. Research, v. 64, p. 1104-1105.

Hietanen, Anna, 1938, On the petrology of the Finnish quartzites: Comm. géol. Finlande Bull. 122, 118 p.

Ingerson, Earl, and Tuttle, O. F., 1945, Relations of lamellae and crystallography of quartz and fabric directions in some deformed rocks: Am. Geophys. Union Trans., v. 26, p. 95-105.

McIntyre, D. B., and Turner, F. J., 1953, Petrofabric analysis of marbles from mid-Strathspey and Strathavon: Geol. Mag., v. 90, p. 225-240.

Naha, Kshitindramohan, 1959, Time of formation and kinematic significance of deformation lamellae in quartz: Jour. Geology, v. 67, p. 120-124.

Riley, N. A., 1947, Structural petrology of the Baraboo quartzite: Jour. Geology, v. 55, p. 453-475.

Saha, A. K., 1955, Deformation-lamellae in quartz from granophyric granite and diorite of Butgora-Sarjori area, eastern Singhbhum [abs.]: Indian Sci. Cong., 42nd, Calcutta, Proc., pt. 3, p. 184.

Schmidt, Walter, 1927, Untersuchungen über die Regelung des Quarzgefüges kristallinger Schiefer: Fortschr. Mineralogie, v. 11, p. 27-29.

Turner, F. J., 1953, Nature and dynamic interpretation of deformation lamellae in calcite of three marbles: Am. Jour. Sci., v. 251, p. 276-298.

Turner, F. J., and Ch'ih, C. S., 1951, Deformation of Yule marble: part III, observed fabric changes due to deformation at 10,000 atmospheres confining pressure, room temperature, dry: Geol. Soc. America Bull., v. 62, p. 887-905.